16th World Conference on Earthquake, 16WCEE 2017

Santiago Chile, January 9th to 13th 2017

Paper N° 2949 (Abstract ID)

Registration Code: S-N1464625064

THE IMPACT OF LONG DURATION EARTHQUAKE ON THE RESPONSE OF MULTI-STOREY CONCENTRICALLY BRACED FRAME BUILDINGS

A. Jnaid(1), L. Tirca(2), A. Bagchi(3)

(1)*PhD student, Department of Building, Civil & Environmental Eng., Concordia University, Montreal, Canada, aidjnaid@gmail.com*
(2)*Associate Prof., Department of Building, Civil& Environmental Eng., Concordia University Montreal, lucia.tirca@concordia.ca*
(3)*Associate Prof., Department of Building, Civil & Environmental Eng., Concordia University, Montreal, ashutosh.bagchi@concordia.ca*

Abstract

Concentrically braced frame (CBF) buildings are widely considered in seismic zones. Although the seismic behavior of CBF systems was extensively studied under the effect of crustal ground motions, the impact of long duration mega-thrust subduction earthquake on the building response is mostly unknown. It is noted that buildings in western Canada (B.C.) are prone to crustal earthquakes and the mega-thrust Cascadia subduction earthquake with a predicted magnitude in the range of 8 to 9 and a mean recurrence period in the range of 500-600 years. From historical references, it was found that the last subduction event was in 1700. The characteristics of subduction versus crustal ground motions vary in terms of amplitude, Trifunac duration and frequency content. Thus, in order to investigate the performance of CBF buildings in Victoria, the best available proxy to a future Cascadia event are the main-shock records from the magnitude 9 Tohoku, Japan earthquake of March 11, 2011 that show several loading/unloading cycles that occured in approximately 300 s. However, the current National Building Code of Canada and Design standards do not require accounting for the number of ground motion cycles for designing earthquake-resistant buildings. Hence, multi-storey buildings designed to withstand the effects of crustal earthquakes may exhibit severe damage under the potential Cascadia subduction earthquake.

In this study, the effect of mega-thrust subduction earthquake on the seismic response of moderately ductile concentrically braced frame multi-storey office buildings located on Site Class C (firm soil) in Victoria, B.C., Canada is investigated from brace yielding to brace fracture caused by low-cycle fatigue. Using data from the 2011 M9 Tohoku subduction earthquake in Japan, nonlinear dynamic analyses were performed on detailed numerical models developed in OpenSees. It was found that the effect of Trifunac duration on the nonlinear seismic response of buildings is particularly significant in terms of the strain accumulated in the fibers of hollow structural section braces, HSS, causing low-cycle fatigue fracture. Mapping the level of damage versus ranges of building height (e.g. 2-storey, 4-storey and 8-storey) it provides an image of building safety. It was found that particular attention should be given when designing low-rise buildings with a fundamental period lower than 0.35 s located in the proximity of subduction fault, such as buildings in Victoria that lie within the Cascadia subduction zone.

Keywords: long duration subduction earthquake; concentrically braced frame; damage index; strain; brace fracture life.

1. Introduction

Concentrically braced frames (CBF) are widely used in North America and are designed to resist gravity, wind, and earthquake loads in agreement with the current code and standard provisions.

Studies have shown that under severe seismic events, CBFs are prone to excessive interstorey drift concentrated within a single floor; have a limited ability to redistribute damage across the structure height and experience lateral strength degradation after braces have buckled. Thus, in order to mitigate these deficiencies, building height limitation and minimum lateral resistance requirements have been introduced in the Canadian Standard, CSA/S16 [1] and the National Building Code of Canada 2010 edition (NBCC) [2]. Braces' response is unsymmetrical after braces buckled in compression. Notwithstanding their robust stiffness, CBFs are prone to concentrate the lateral forces and deformations within a floor that consequently leads to the formation of a soft storey mechanism. In addition, the redistribution of internal forces and lateral deformations is strongly influenced by the frequency contents of ground motions.

The building stock in western Canada, (e.g. Victoria, BC) is subjected to crustal and Cascadia subduction ground motions. Recent investigations have revealed that the distance to the fault of Victoria and Vancouver is less than 120 km [3]. According to data posted on earthquakescanada.nrcan.gc.ca website, Cascadia subduction thrust-fault mechanism is due to the landward and beneath to the continent movement of the Juan de Fuca plate at an average speed of 40 mm/year. On the West-East axis, Juan de Fuca plate lies between the Pacific plate and the North American plate, while on the North-South axis it lies between the Vancouver Island and northern California. The Cascadia thrust-fault produces rare and large magnitude earthquakes that may reach a magnitude of M9 and the epicentre may occur in the vicinity of Victoria. The recurrence period for the Cascadia subduction earthquake is approximately 500 years. Likewise for the magnitude M9 Japan Tohoku earthquake [4], Cascadia records are estimated to be characterized by long duration and high frequency content.

The purpose of this resaerch is to investigate the behaviour of multi-storey concentrically braced frame buildings located on firm soil in Victoria, BC, when subjected to a set of crustal versus subduction ground motions, likely Tohoku records.

2. Building Description

2.1 Building geometry

In this study, a prototype 2-storey, 4-storey and 8-storey CBF office buildings were selected for investigation. All buildings have the same plan layout as shown in Fig. 1a. In the East-West (E-W) direction, the building is braced by four CBFs in chevron bracing configuration and in the North-Soudth (N-S) direction there are two CBFs of two adjacent bays each. These CBFs have diagonal tension-compression braces made of square hallow structural sections (HSS). The CBFs of studied buildings located in the N-S direction (e.g. gridline B) are shown in Fig. 1b and are analysed here. At the roof level, the dead load is 4.1 kPa and at the typical floor is 5.1 kPa. The live load for the typical floor is 2.4 kPa and the snow load is 1.08 kPa. For cladding, 1.0 kPa was considered. The building was designed according to the CSA/S16-2009 standard [1] in conjunction with the requirements of the NBCC [2]. Accordingly, the static seismic base shear, *V*, is:

$$V = \frac{S(T_a)M_v I_E W}{R_d R_0} \tag{1}$$

where $S(T_a)$ is the design spectral acceleration corresponding to the fundamental period of the building which is estimated as $T_a = 0.025h_n$ and h_n is the building height. Herein, M_v is the higher mode factor, I_E is the importance factor, R_d is the ductility-related force modification factor and R_o is the overstrength-related force modification factor. The 2-storey, 4-storey and 8-storey office buildings are located on a firm soil in Victoria, B.C. and are classified as normal importance category. The spectral acceleration values for Victoria at the period of 0.2, 0.5, 1.0 and 2.0 s are equal to 1.2, 0.82, 0.38 and 0.18 g, respectively, where g is the gravitationl acceleration. In this study, the CBF systems were considered moderately ductile with R_d = 3 and R_o = 1.3. When dynamic analysis is employed, a maximum fundamental period of $2T_a$ could be considered for the calculation of static base shear. If from dynamic analysis it results a first-mode vibration period T_1 between T_a snd $2T_a$, the T_1

is used in design. However, the value of the computed static base shear V should not be larger than the maximum base shear V_{max}, where $V_{max} = 2/3(S(0.2)M_v I_E W/R_d R_o)$, and not lower than $V_{min} = S(2.0)M_v I_E W/R_d R_o$. To be qualified as a regular building, all irregularities criteria were checked. Among them, the torsional sensitivity criterium for regular buildings requires that parameter B at any storey in the direction of loading to be lower than 1.7, where $B = \delta_{ave}/\ \delta_{max}$. Herein, δ_{ave} is the average displacement of the structure due to torsion at level x and δ_{max} is the maximum displacement due to torsion at the same floor level. It resulted that all studied buildings are

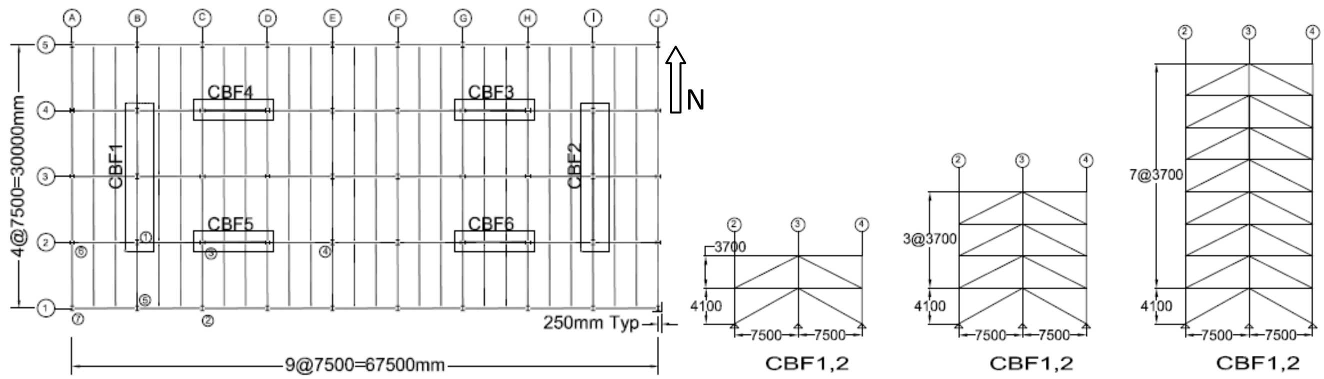

regular.

Fig. 1 - Building plan and CBF elevations of 2-storey, 4-storey, and 8-storey buildings in the N-S direction

All CBFs beams and columns cross-sections are made of W-shape and all braces are made of HSS with F_y = 350 MPa. These CBF members are designed as Class 1 sections and are proportioned to carry the seismic load in combination with the gravity load. The first-mode period obtained from nonlinear dynamic analysis using OpenSees [5] is similar to $2T_a$. The fundamental period computed with the code equation ($2T_a$), the period of the buildings in the first two modes (T_1 and T_2) resulted from the OpenSees output, the building seismic weight W and the associated design base shear as per dynamic analysis, V_d are given in Table 1. The CBF members sizes resulted from design are showed in Table 2. To complay with the serviceability criterium, the peak interstorey drift should be within the code limit of $2.5\%h_s$, where h_s is the storey height.

Table 1- Buildings dynamic characteristic

Building type	$2T_a$ (s)	T_1 Nonlinear dyn. analysis	T_2 OpenSeees (s)	W (kN)	V_d (kN)
2-storey	0.39	0.38	0.16	19537	4008
4-storey	0.76	0.69	0.26	40812	6488
8-storey	1.50	1.40	0.49	81904	5880

Table 2 - Members sizes

Fl.	Brace[a]	Beam	Mid Col.	Side Col.	Brace[a]	Beam	Mid Col.	Side Col.
8	52x9.5	W360x64	W360x122	W360x79				
7	178x13	W360x106	W360x122	W360x79				
6	203x13	W360x106	W360x237	W360x147				
5	203x13	W360x128	W360x237	W360x147				
4	228x13	W360x128	W360x382	W360x262	178x13	W360x79	W360x110	W360x91
3	228x13	W360x144	W360x382	W360x262	203x13	W360x79	W360x110	W360x91
2	254x13	W360x144	W360x551	W360x347	254x13	W360x110	W360x179	W360x179
1	254x13	W360x144	W360x551	W360x347	254x13	W360x110	W360x179	W360x179

	Brace[a]	Beam	Mid Column	Side Column
2	254x13	W360x110	W360x122	W310x91
1	203x9.5	W360x72	W360x122	W310x91

2.2 Ground motion selection and scaling

The current building code requires that the selected ground motions to be scaled to match the uniform hazard spectrum for Victoria (UHS) computed as 2% per 50 years probability of exceedance. For Site Class C (firm soil), the UHS corresponds to design spectrum, DS. More specifically, Site Class C is defined when the average shear wave velocity $\overline{V}_s$ in the top 30 m layer is in the range of 360 m/s < $\overline{V}_s$< 760 m/s. In this study, two sets of seven ground motions each comprising records from crustal and subduction earthquakes were selected. The methodology applied to ground motions' scaling complies with the ASCE/SEI 7-10 procedure [6]. Hence, this methodology requires that the mean of a minimum seven scaled ground motions to match or be above the design spectrum over the period of interest $0.2T_1$ - $1.5T_1$.

The set of seven crustal records were selected from M6.7-M6.9 Californian earthquakes, and the subduction ground motion set comprises seven records from the mega-thrust M9 Tohoku earthquake (March 11 2011, Japan). All records were selected to match the geotechnical profile for Site Class C in Victoria, BC. These ground motions are shown in Table 3 together with the peak ground acceleration, PHA, peak ground velocity, PGV, the total duration, t, the Trifunac duration, t_d, the predominant period T_p and the main period T_m of ground motions, respectively. Among the seven crustal ground motions, six have a total duration of 40 s and one has 60 s, the average of the Trifunac duration is 11.3 s, the average of shear wave velocity is 424 m/s with a minimum value of 360 m/s and a maximum value of 489 m/s. In addition, the average velocity and acceleration of selected crustal records is 0.28 m/s and 0.33 g, respectively, while the average value of the predominant and mean period is 0.21 s and 0.53 s. In comparison with Tohoku records, the later show large duration of 300 s and an average Trifunac duration of 67 s which is six times longer than that of crustal record set. The average shear wave velocity is in the same range as that computed for the crustal record set, while the average value of velocity and acceleration that corresponds to selected records of magnitude 9 Tohoku earthquake is larger: 0.39 m/s and 0.8 g, respectively. However, Tohoku records are characterized by high frequency with an average T_p and T_m value of 0.25 s and 0.19 s, respectivelly. In comparison with the crustal records, the predominant periods of the Tohoku records are in the same range. It is noted that the selected S1, S2, S3 records are characterized by a combination of two wave shapes arising from the propagation of rupture along the shore, while the others are characterized by a single wave similar to crustal records.

Table 3- Characteristics of selected ground motions

No.	Event	M	Station	R_{hyp} [3] (km)	Cmp. (^{0})	PHA (g)	PHV (m/s)	t; t_d (s)	T_p; T_m (s)
			Subduction ground motions[1]						
S1	03/11, 2011Tohoku	9	MYG001	155	EW	0.43	0.23	300; 83	0.27; 0.26
S2	03/11, 2011Tohoku	9	MYG004	184	EW	1.22	0.48	300; 85	0.26; 0.25
S3	03/11, 2011Tohoku	9	FKS005	175	EW	0.45	0.35	300; 92	0.32; 0.15
S4	03/11, 2011Tohoku	9	FKS010	189	EW	0.86	0.56	300; 66	0.27; 0.18
S5	03/11, 2011Tohoku	9	FKS009	216	EW	0.83	0.44	300; 74	0.20; 0.20
S6	03/11, 2011Tohoku	9	IBR004	273	EW	1.03	0.38	300; 33	0.21; 0.15
S7	03/11, 2011Tohoku	9	IBR006	283	EW	0.78	0.30	300; 36	0.25; 0.12
			Crustal ground motions[2]						
C1	01/17, '94, Northr.	6.7	Castaic Old Ridge R	44	90	0.57	0.52	45; 9.10	0.26; 0.54
C2	01/17, '94 Northr.	6.7	LA, UCLA Grounds	25	90	0.28	0.22	60; 11.3	0.22; 0.34
C3	01/17, '94, Northr.	6.7	Moorpark – Fire St.	36	180	0.29	0.20	40; 14.2	0.26; 0.47
C4	10/18, 1989 L.P.	6.9	Gilroy Array #3	36	0	0.56	0.36	39.9; 6.4	0.20; 0.37
C5	10/18, 1989, L.P.	6.9	Palo Alto, SLAC Lab	54	360	0.28	0.29	39.6;11.6	0.30; 0.65
C6	10/18, 1989, L.P.	6.9	Apeel 9, Crystal Sp.	41	227	0.11	0.18	40; 16.2	0.30; 0.88
C7	10/18, 1989, L.P.	6.9	Anderson Dam, DS	20	250	0.25	0.20	40; 10.4	0.20; 0.46

1) Subdaction ground motions were selected from: www.k-net.bosai.go.jp
2) Crustal ground motions were selected from: http://peer.berkeley.edu/peer_ground_motion_database/
3) In this table, only the hypocentral distance is reported, not the distance to the fault.

The acceleration response spectrum of scaled crustal and subdaction records are illustrated in Fig. 2 together with the mean value of minimum seven records and the design spectrum as required by NBCC 2010 for Victoria, BC. The acceleration response spectrum obtained from the selected Tohoku records show very large ordinates in the short period range 0.1 - 0.35 s. Thus, low-rise buildings with a fundamental period in this range may be exposed to ground motions that are about three times larger than those required by the code. However, buildings with a fundamental period larger than 0.8 s are not exposed to increased acceleration response spectrum ordinates. For all subduction records the scale factor was not raised above 1.0 although in some intervals the average spectrum is slightly lower than that required by the building code. Regarding crustal records, computed scaling factors were applied.

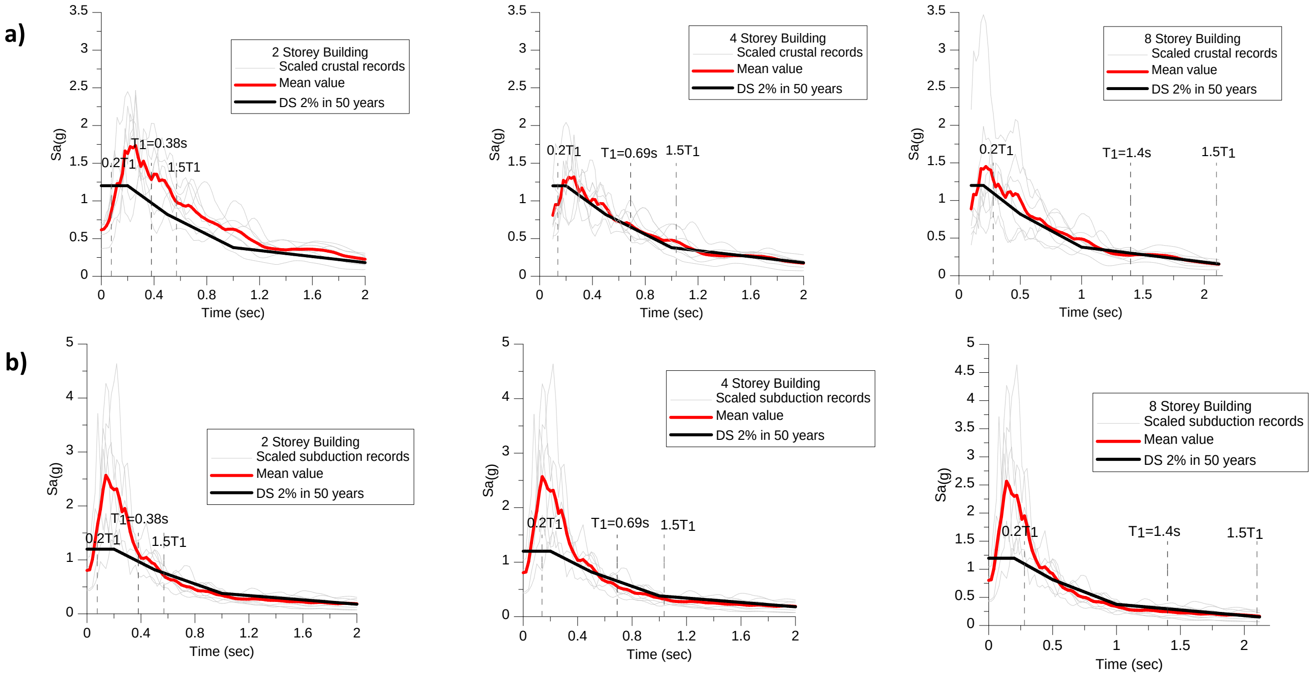

Fig. 2 - Scaled acceleration response spectrum for studied building: a) crustal records, b) subduction records

3. Numerical Model

Due to building's symmetry, the OpenSees model was built for half of building's floor plan and the direction of seismic loading considered in this study is N-S. The model illustrated in Fig. 3a was developed to allow the out-of-plane deformation of HSS braces. Each CBF brace was modeled with twenty nonlinear beam-column elements with distributed plasticity displaced across the member length and 4 integration points per element. The HSS brace member's cross-section was meshed with rounded corners and comprises 200 fibers as shown in Fig. 3b. To allow braces to backle out-of-plane an initial camber of $L/500$, where L is the length of the brace, was assigned in the out-of-plane direction. *Steel02* material with isotropic strain hardening known as Giuffre-Menegotto-Pinto material was assigned to all CBF brace and column members. All CBF beams were pinned-connected to columns and were modeled as elastic beam-column elements. Columns are continuous over two floors and are pinned at the base. Both beam and column members are made of W-shape with F_y = 350 MPa. Each column member was modeled with eight nonlinear beam-column elements, 4 integration points per element and an initial camber of $h_s/1000$, where h_s is the storey height. The column's W-shape cross-section was made of 80 fibers distributed equally between the flanges and the web. Gravity columns were modeled as elastic beam-column elements. Braces were connected to the frame by means of gusset plate connections. The properties of gusset plate connections were replicated by assigning two rotational and one torsional spring in the *zero-length* element located between each end of the brace member and a rigid link member [7]. The out-of-plane flexural stiffness of the gusset plate is EI/L_{ave}, where L_{ave} is the average of L_1, L_2 and L_3 dimensions illustrated in Fig. 3b and I is the moment of inertia computed as: $I = B_w t_g^3/12$. Herein, B_w is the Whitmore width which is defined by the 30° projection angle, t_g is the thickness of the gusset plate and E is the elastic modulus.

The in-plane flexural stiffness of the gusset plate was computed to be greater than the brace stiffness. A third torsional spring assigned in the *zero-length* element considered the torsional stiffness of the gusset plate defined as GJ/L_{ave},where G is the shear modulus of steel material and J is the torsional constant given by: $J = 0.333B_w t^3$. Both flexural springs were made of *Steel02* material and the torsional spring of elastic material.

From experimental testing it was found that HSS brace fracture occurs at brace's mid-span where the plastic hinge is formed. At this location, cracks are propagated after the occurrence of local buckling and the fracture mechanism is cause by the low-cycle fatigue. To simulate this effect, Uriz [8] proposed and developed in OpenSees the *fatigue material* model defined by two parameters ε_0 and m, where ε_0 is the strain for a single reversal and m is the fatigue ductility exponent. This model used accumulative strain to predict damage in accordance with Miner's rule and the modified rainflow cyclic counting method. Thus, *fatigue material* is wrapped around the brace's parental material *Steel02* and when a fiber of HSS brace cross-section reaches its fatigue life (Damage Index =1), its stress and stiffness fall to zero. A constant set of *fatigue material* parameters were proposed in [8]. However, using this set of constant parameters, it was found that several experimental tests could not be aqurately replicated. To solve this drawback, Tirca and Chen [9] proposed the following *fatigue material* parameters for HSS braces with the slenderness ratio KL/r between 50 and 150:

$$\varepsilon_{0pred} = 0.006\left(\frac{KL}{r}\right)^{0.859}\left(\frac{b_0}{t}\right)^{-0.6}\left(\frac{E}{F_y}\right)^{0.1} \text{ and m = -0.5} \qquad 2$$

Eq. (2) was calibrated against 14 experimental tests from the literature. Herein, b_0/t is the width-to-thickness ratio calculated as $(b-4t)/t$ [1] where b and t are the HSS dimension and thickness, respectively. The 3% Rayleigh damping proportional to the initial stiffness was assigned to the first and second mode of vibration for the 2-storey building, and the first and third mode of vibration for the 4-storey and 8-storey buildings.

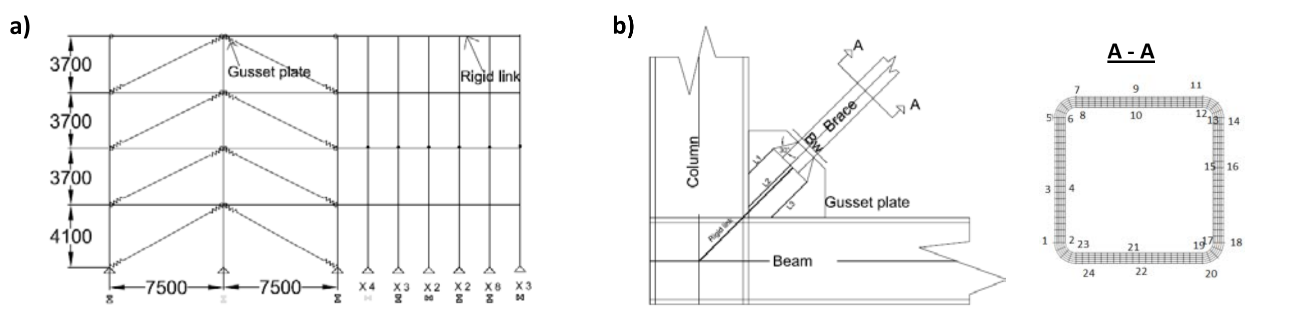

Fig. 3 - OpenSees model for the 4-storey building: a) elevation, b) brace-to-frame connection detail

4. Numerical Results

To emphasize the differences in the nonlinear response of multistory moderately ductile CBF buildings subjected to subduction versus crustal records, the following response parameters were investigated: interstorey drift, residual interstorey drift, strain developed in the tensile and compressive fiber of HSS brace cross-sections at the critical location of plastic hinge formation and the associated accumulated strain.

In Fig. 4 it is shown the maximum inter-storey drift ($\delta_{max}\%h_s$), the median and 84% percentile for the 2-storey, 4-storey, and 8-storey building under both sets of crustal and subduction ground motions. Thus, in the case of 2-storey building the maximum interstorey drift occurs under the crustal ground motion set. The maximum interstorey drift demand occurred at the top floor where the median value was about 0.69%h_s for the subduction ground motion set and 0.99%h_s for the crustal ground motion set. In the case of 4-storey building, the maximum interstorey drift demand occurred at the bottom level under both crustal and subduction records. Hence, the median value is 0.65%h_s and 0.73%h_s under the crustal and subduction record set, respectively. For the 8-storey building the maximum interstorey drift demand occurred at the upper two floors where the median interstorey drift is 1.9%h_s and 1.59%h_s under the crustal and subduction record set, respectively. It is noted that the peak of the 84% percentile is 2.33%h_s under the effect of crustal records and 1.88%h_s under subduction records. However, under the effect of subduction records characterized by high frequency, an increase in interstorey drift was observed between the 2nd and 4th floor level.

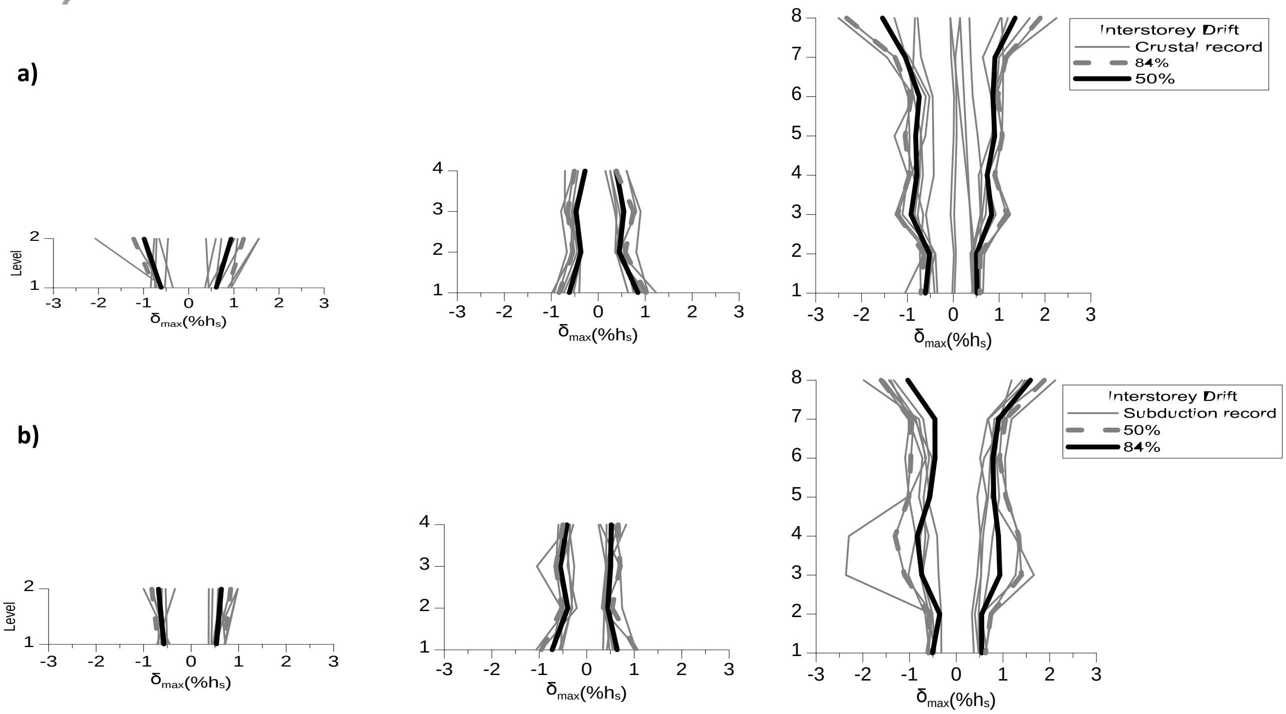

Fig. 4 - Interstorey drift demand for the 2-, 4- and 8-storey building: a) crustal records, b) subduction records

Figure 5 shows the maximum residual interstorey drift across the building height ($\delta_{r,max\%}h_s$), the median and 84% percentile for the 2-, 4- and 8-storey buildings under the crustal and subduction ground motion sets. In the case of 2-storey building, the maximum residual inter-storey drift, $\delta_{r,max}\%h_s$ occurred at the top floor under both sets of ground motions. The 50% and 84% percentile of residual interstorey drift recorded at the top floor under the crustal record set is 0.1%h_s and 0.19%h_s, respectively while under the subduction record set is 0.06%h_s

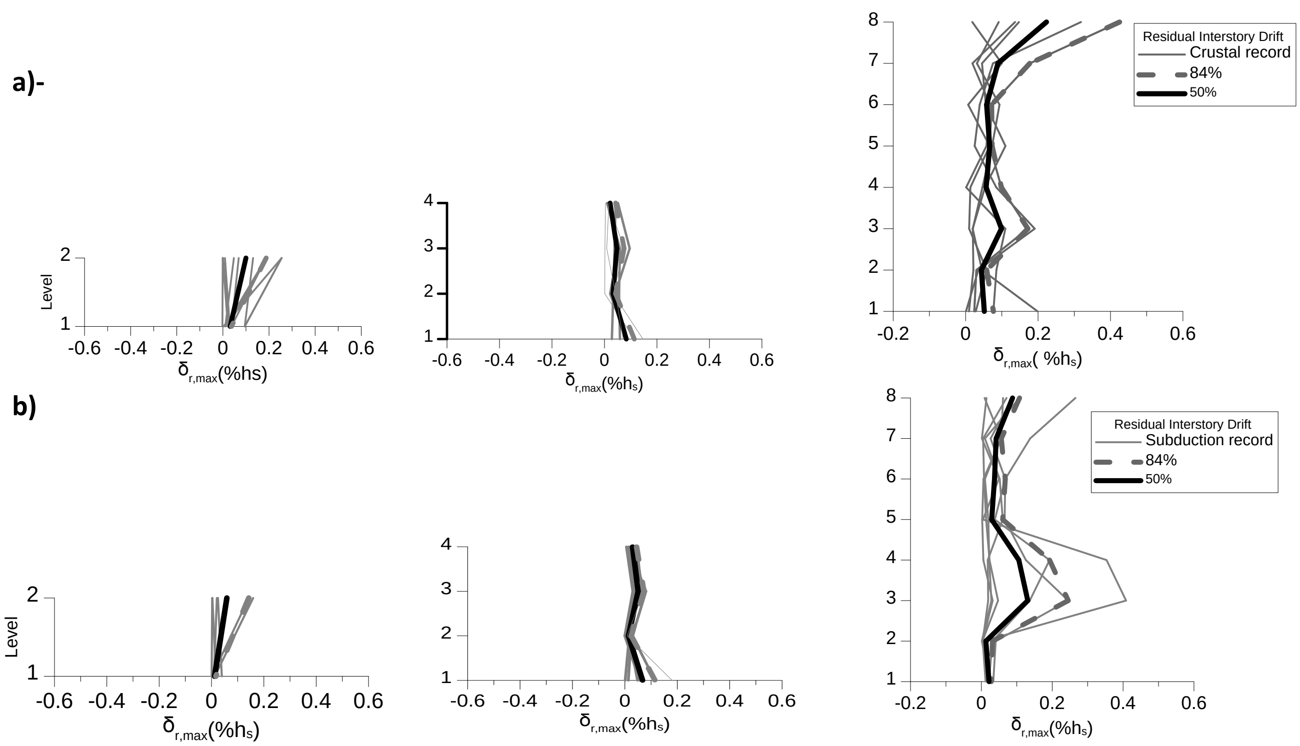

Fig. 5 - Residual interstorey drift demand for 2-, 4-, 8-storey buildings: a) crustal records, b) subduction records

and 0.142%h_s, respectively. For the 4-storey building, the maximum residual interstorey drift demand occured at the ground floor where the 50% and 84% percentile is 0.083%h_s and 0.114%h_s, respectively under the crustal record set versus 0.068%h_s and 0.115%h_s under the subduction record set. For the 8-storey building, the maximum residual interstorey drift demand occurred at the top floor under the crustal records where the median residual interstorey drift is 0.223%h_s and the 84% percentile is 0.425%h_s. When the 8-storey building was subjected to subduction record set, the peak of the 84% percentile is 0.245%h_s and was recorded at the 3rd floor. Among the 7 subduction records, the maximum residual interstorey drift of 0.408%h_s occurred at the 3rd floor under the FKS005EW record.

The ductile fracture of HSS braces cause by low–cycle fatigue is the desirable failure mode of CBF structures [7]. In order to investigate the HSS brace's fracture life, the accumulated strain in the outermost compressive fibre of the HSS brace's cross-section is a good indicator. Herein, the low-cycle fatigue material assigned to HSS braces was defined by using the fatigue material parameters given in Eq. (2). Then, the strain developed during earthquake loading was recorded in each fiber of the HSS brace cross-section (Fig. 3b). In OpenSees, the number of cycles was counted by using the modified rainflow counting algorithm. According to [10], the damage index, DI, denotes the ratio between the current number of cycles and the maximum number of cycles permitted by Coffin and Manson's fatigue theory. When DI of monitored fiber reaches 1.0, the fiber is disconnected. Further, when all fibers within a critical brace's cross-section reached DI = 1.0, the HSS brace exhibits fracture and the brace is disconnected from the CBF.

Fig. 6 shows the level of damage developed in the outermost compressive fiber of HSS braces at their critical cross-sections. Hence, DI associated to brace's cross-section was computed for the 2-, 4- and 8-storey CBFs subjected to crustal and subduction records. As depicted, the largest strain accumulated in the HSS brace's cross-section fibers occurs at floors experiencing the peak interstorey drift. Due to large Trifunac duration comprising several loading/ unloading cycles, the fracture life of HSS braces is shorter when sbuduction records are used. In the case of 2-storey building, the top floor braces are likely to fracture first. The 84% percentile of DI is 78% under the subduction records versus 35% under crustal records. It is noted that in one case the HSS brace reached fracture under the MYG004 record. In the case of 4-storey building the lagest damage occurs at bottom floor where the 84% percentile DI corresponds to 60% under the subduction records versus 19% under crustal records. For the 8-storey building the largest damage under crustal records occurred at the top floor (84% percentile of DI = 17%) and under the subduction records at the 3rd floor where 84% percentile of DI = 52%.

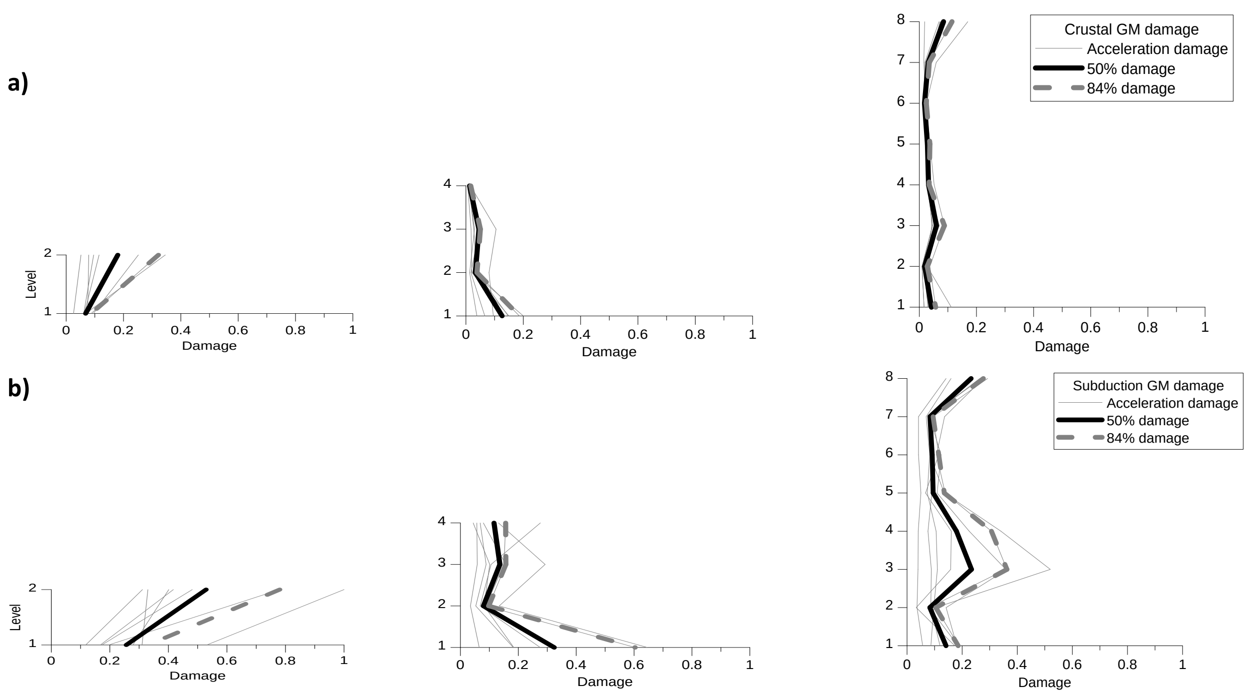

Fig. 6 - DI at critical brace cross-sections of the 2-, 4-, 8-st. buildings: a) crustal records, b) subduction records

5. Case studies

5.1 Nonlinear response of 2-storey CBF building

Detailed nonlinear response of the 2-storey CBF building subjected to Tohoku subduction record S2 and crustal Northridge record C3 is shown in Fig. 7 in terms of: time-history roof drift (%H); time-history interstorey drift of top floor where the larger damage was triggered; hysteresis response of the right and left HSS braces located at top floor and the associated time-history strain developed in the outermost compression and tensile fibers of critical cross-section; as well as the computed damage index. From Fig.7 resulted that the roof drift under both records is within the code limits ($\leq$ 2.5%h_s), where the roof drift was calculated by dividing the roof displacement to the building height. As depicted in Fig. 7, both left and right HSS braces located at the top floor exhibited fracture caused by low-cycle fatigue under the S2 record. It is noted that under both records braces buckled in compression and reached yielding in tension. Time-history strain series recorded in the outermost

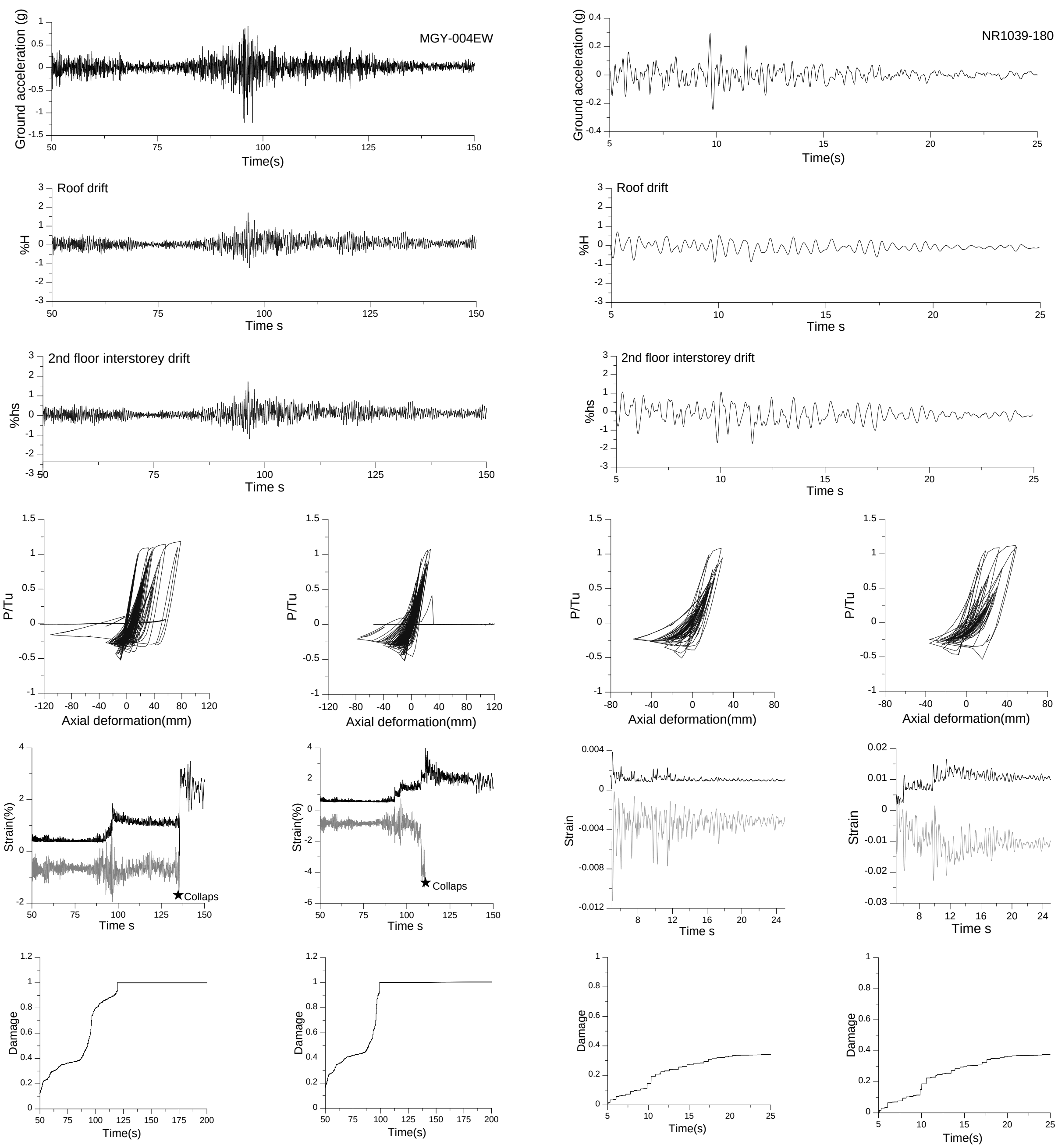

Fig. 7 - Nonlinear response of 2-storey CBF building under the S2 subduction and C3 crustal records

compression fibers of critical HSS brace cross-section shows larger amplitudes under the subduction record than the crustal record. As illustrated in Fig. 7, the damage index computed for the left and right HSS braces located at top floor shows DI = 1.0 at failure and DI < 1.0 in case of crustal record.

5.2 Nonlinear response of 4-storey CBF building

The comparison of seismic response of the 4-storey building subjected to S4 Tohoku record and C5 Loma Prieta record is showed in Fig. 8. It is noted that the scaling factors for the S4 and C5 records are 1.0 and 1.39, respectively.The response of the building at the bottom floor level was recorded. As illustrated, the roof drift, %H and the interstorey drift, %h_s are slightly bigger under the crustal than subduction record. The hysteresis response of the right and left HSS braces located at ground floor experienced buckling in compression and yielding in tension under both crustal and subduction records but did not reach fracture. The associated time-hystori strain series recorded in the same braces under the crustal and subduction records show large amplitude

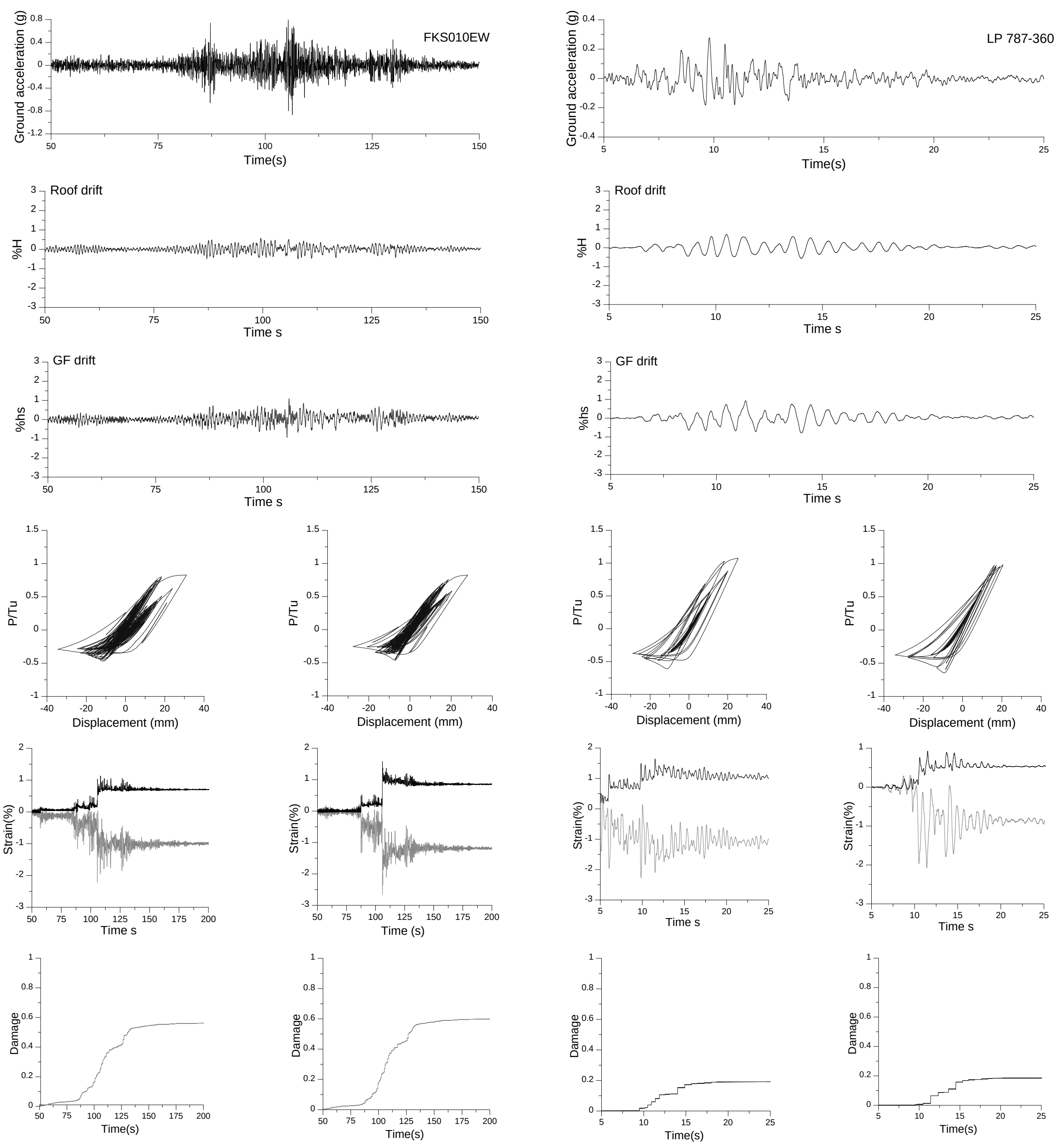

Fig. 8 - Nonlinear response of 4-storey CBF building under the S4 subduction and C5 crustal records

strain triggered in the outermost compressive fiber under both crustal and subduction records. However, under the subduction record effect, it resulted DI = 60% versus 20% damage under the crustal record effect.

5.3 Nonlinear response of 8-storey CBF building

In the case of 8-storey building, the investigation was conducted under the S3 Tohoku subduction record and the C7 Loma Prieta crustal record. A scaling factor of 1.0 was applied to S3 record and 1.5 to C7 record. The larger demand occured at the top floor. As illustrated in Fig. 9, the roof drift %H and roof interstorey drift %h_s are slightly larger under the crustal than subduction record. The left and right HSS braces located at the top floor reached their tensile strength under both records. However, larger amount of energy is dissipated by the right brace than the left brace under both crustal and subduction ground motions. The time-hystori strain series was recorded for the outermost compression and tension fiber of both left and right brace's critical cross-section. The maximum strain amplitudes are similar under both records. However, the associated DI is equal to 53% under the subduction record and only 17% under the crustal record. Similar findings were reported in [10].

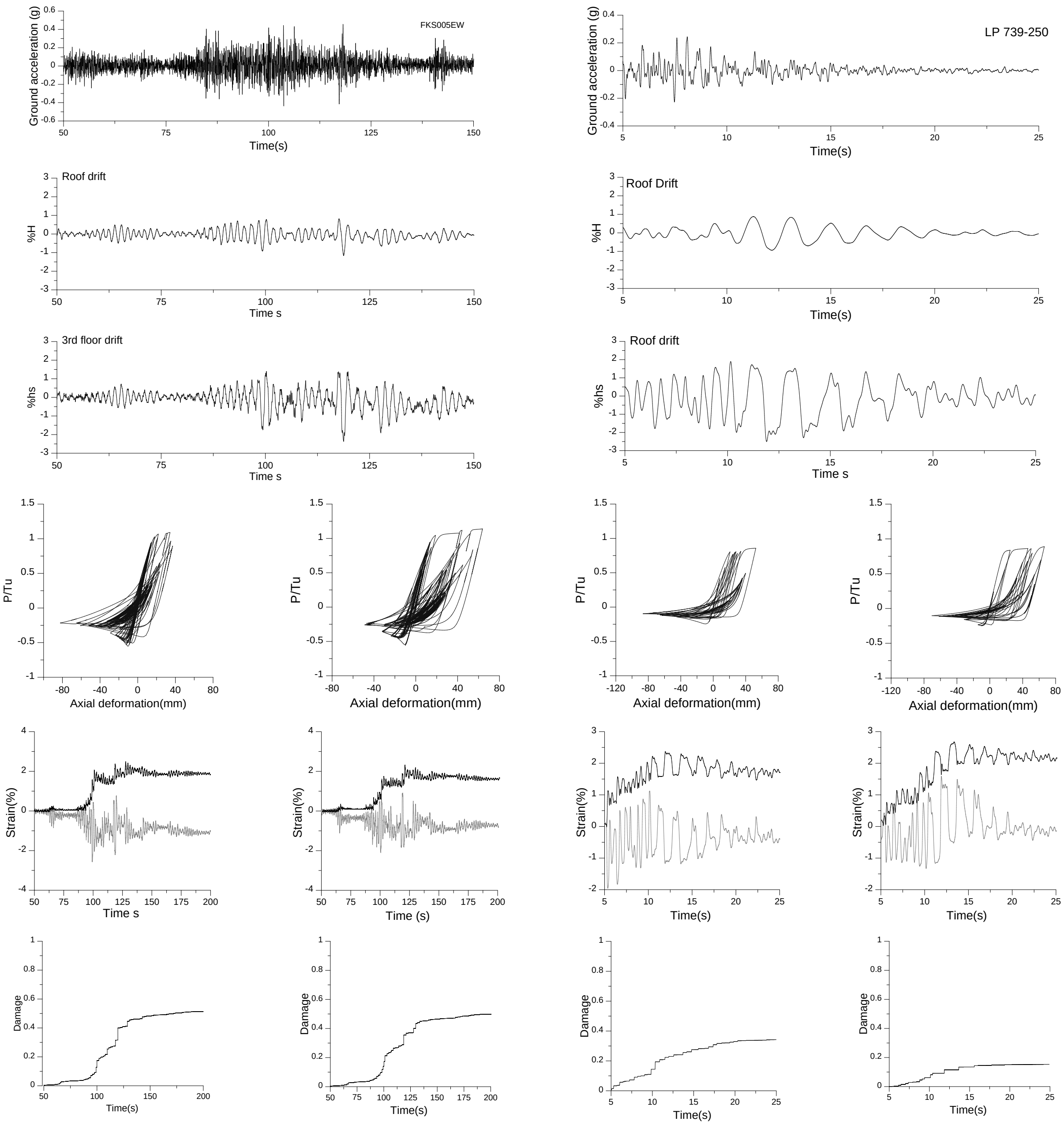

Fig. 9 - Nonlinear response of 8-storey CBF building under the S3 subduction and C7 crustal records

6. Conclusions

The nonlinear behaviour of the 2-storey, 4-storey and 8-storey moderately ductile CBF buildings located in Victoria was analysed under two sets of ground motions: crustal and subduction. The CBF model was developed in OpenSees and the investigated parameters are: interstorey drift, residual interstorey drift, damage index computed for HSS braces. The latter was expressed as the ratio between the current number of cycles and the maximum number of cycles permitted by Coffin and Manson's fatigue theory. The findings of this study are:

- All subduction records are from the mainshock M9 Tohoku earthquake characterised by longer Trifunac duration and several loading/ unloading cycles. All records were selected to match the geotechnical profile for Site Class C in Victoria, BC. For subduction records a scaling factor equal to 1.0 was considered, while a computed scaling factor was applied to crustal ground motions. The shape of subduction accelerograms that captured two adjacent seismic waves (e.g. MYG004 record) did not seem to have a special effect on the behaviour of buildings. However, in the short period range (T < 0.35 s), the magnitude of acceleration response spectrum ordinates are about 3 times greater than the code demand. Hence, the top floor HSS braces of the 2-storey building experiend low-cycle fatigue fracture. Thus, buildings characterized by a first-mode period lower than 0.35 s are exposed to high seismic risk.
- For all studied buildings, the main demand occured either at the top or upper two floors or at the bottom floor. The interstorey drift of studied buildings are within the code limit of 2.5%h_s. To assess the level of damage, residual interstorey drift was triggered at each floor. In all cases but one (2-storey building subjected to subduction records) it was found $\delta_{r,max}\%h_s < 0.5\%h_s$ which indicates that these buildings are reparable and no a total loss.
- Damage index is a good indicator for the assessment of fracture life of HSS braces. From analysis, it resulted larger brace fracture life when buildings are subjected to crustal versus subduction earthquakes.

7. Acknowledgements

Authors thank Prof. Atkinson and Dr. Ghofrani for providing valuable input on the selection of subduction records.

8. References

[1] Canadian Standard Association, CAN/CSA-S16 (2009). Limit states design of steel structures. Toronto, ON

[2] National Research Council of Canada (2010). National Building Code of Canada – Part 4, Ottawa, ON.

[3] Atkinson G, and Macias M (2009). Predicted ground motions for great interface earthquakes in the Cascadia subduction zone. *Bulletin of the Seismological Society of America*, 99(3), 1552-1578.

[4] Ghofrani H, Atkinson G, Goda K (2012): Implications of the 2011 M9.0 Tohoku Japan earthquake for the treatment of site effects in large earthquakes. *Bulletin Earthquake Engineering*.

[5] McKenna F, Fenves G, Scott M, et al. (2015): Open system for earthquake engineering simulation. Opensees software version 2.4.5. PEER, University of California, Berkeley.

[6] American Society of Civil Engineers (ASCE) (2010): Minimum design loads for buildings and other Structures. *ASCE/SEI 7-10*, Reston, Virginia.

[7] Hsiao PC, Lehman D, Roeder C (2012): Improved analytical model for special concentrically braced frames. *Journal of Constructional Steel Research*, 73:80-94.

[8] Uriz P (2005): Towards earthquake resistant design of concentrically braced steel buildings. *Ph.D. Dissertation*, University of California, Berkeley.

[9] Tirca L, Chen L (2014): Numerical simulation of hollow structura teel braces upon fracture. *Journal of Advanced Steel Construction.* 10(4) (2014)442-462.

[10] Tirca L, Chen L, Tremblay R (2015): Assessing collapse safety of CBF buildings subjected to crustal and subduction earthquakes. *Journal of Constructional Steel Research.* 115: 47-61.